Food and Bioprocess Technology (2024) 17:2782–2792
https://doi.org/10.1007/s11947-023-03266-z

RESEARCH

A New Index to Detect Process Deviations Using IR Spectroscopy and Chemometrics Process Tools

Daniel Schorn-García[1] · Jokin Ezenarro[1] · Olga Busto[1] · Laura Aceña[1] · Ricard Boqué[1] · Montserrat Mestres[1] · Barbara Giussani[2]

Received: 5 June 2023 / Accepted: 14 November 2023 / Published online: 19 December 2023

Abstract
Process analytical technologies (PATs) have transformed the beverage production management by providing real-time monitoring and control of critical process parameters through non-destructive measurements, such as those obtained with infrared (IR) spectroscopy and enabling process readjustment if necessary. New requirements in the analysis of beverages call for new methods, so in this article, we propose a method based on the construction of multivariate statistical process control (MSPC) charts from a new dissimilarity index (the evolving window dissimilarity index, EWDI) to monitor fermentation processes. The EWDI was applied to monitor wine alcoholic fermentation, the biochemical transformation of sugars into ethanol. Small-scale fermentations were carried out and analyzed using a portable mid-infrared spectrometer. In some of them, process deviations due to nitrogen deficiency or temperature changes were intentionally promoted to evaluate the performance of the EWDI. The MSPC charts build by using the fermentations carried out under normal operating conditions allowed identifying deviations of the fermentation in its early stages. Furthermore, the shape of the EWDI curve over time provides insights about the specific type of deviation occurring. These results show the potential of this new approach to improve the monitoring and control of key process stages in biochemical processes in the food industry, which allows maximizing quality and minimizing losses.

Keywords Mid-infrared spectroscopy · Wine · Real-time monitoring · Evolving window principal component analysis (PCA) · Confidence limits · Control chart

Introduction

The beverage industry is a continuously changing sector in which alcoholic beverages have the largest economic contribution (Food Drink, 2022). This implies that the alcoholic beverage industry today faces new challenges related to the different production processes, among which alcoholic fermentation stands out. Alcoholic fermentation is a complex biochemical transformation of sugars into ethanol that can slow down (sluggish fermentation) and even stop (stuck fermentation) for a number of reasons, including inadequate concentration of nutrients or sudden changes in fermentation

✉ Barbara Giussani
barbara.giussani@uninsubria.it

Daniel Schorn-García
daniel.schorn@urv.cat

Jokin Ezenarro
jokin.ezenarro@urv.cat

Olga Busto
olga.busto@urv.cat

Laura Aceña
laura.acena@urv.cat

Ricard Boqué
ricard.boque@urv.cat

Montserrat Mestres
montserrat.mestres@urv.cat

[1] Chemometrics and Sensorics for Analytical Solutions (CHEMOSENS) group, Department of Analytical Chemistry and Organic Chemistry, Universitat Rovira i Virgili, Campus Sescelades, Edifici N4, C/Marcel·lí Domingo 1, Tarragona 43007, Spain

[2] Dipartimento di Scienza e Alta Tecnologia, Università Degli Studi Dell'Insubria, Via Valleggio, 9, 22100 Como, Italy

conditions (Hernández et al., 2016; Urtubia et al., 2008). The slow rate of sugar consumption by the yeasts indicates that their metabolism is not working properly, which can lead to the synthesis of undesirable molecules. These can negatively influence the sensory perception of the final product and, therefore, its quality (Alexandre & Charpentier, 1998).

The possibility of recovering a problematic fermentation depends on early detection of the problem, which allows producers to take corrective measures to minimize the impact on product quality (Nieto-Ortega et al., 2023; Schorn-García et al., 2021). This concept perfectly fits with the implementation of process analytical technologies (PATs). The PAT approach is based on the idea that final product quality is achieved through real-time measurements throughout the process, which allow readjustments while the problem is still solvable, rather than assessing final product quality when the process has already been completed (Jenzsch et al., 2018; Services, U.S. Department of Health and Human, Food and Drug Administration, 2004). The implementation of PAT methodologies in the food and beverage industry requires the acquisition of in- or on-line fast measurements to gather real-time information about the molecules involved in the process. Additionally, the use of non-destructive measurements is recommended, as they can provide valuable information without affecting the quality or composition of the process (Jenzsch et al., 2018). Regarding wine alcoholic fermentation, vibrational spectroscopy (near infrared, mid-infrared, or Raman) has proven to be a useful tool for obtaining process information (Cavaglia et al., 2020a, b; Cozzolino, 2015, 2016, 2022). In these cases, the data being acquired are multivariate, and, therefore, the use of multivariate statistical process control (MSPC) techniques is necessary for fermentation process monitoring and control. Among the different types of MSPC charts, those based on principal component analysis (PCA) are widely used because they are simple and easy to interpret (Nomikos & MacGregor, 1995). However, other approaches such as the prediction of relevant parameters (Bao et al., 2014; Ye et al., 2014) or application of multivariate curve resolution techniques (Grassi et al., 2014; Nieto-Ortega et al., 2023) have also been proposed.

The application of the PCA-based control chart approach involves selecting a reference set that defines the normal operating conditions (NOC) for a particular process, with its intrinsic variability, and comparing future values with this set. Thus, a PCA model is built using NOC data, and future data are projected onto the "NOC" PCA model. Then, the values of model parameters such as Hotelling's T^2 and Q residuals are used to assess whether the new data are compatible with those recorded in the NOC. These parameters provide information about how a particular measurement fits the NOC model. Hotelling's T^2 and Q residuals control charts have been shown to be effective in wine alcoholic fermentation to detect lactic acid bacteria spoilage (Cavaglia et al., 2020a), along with other monitoring strategies (Cavaglia et al., 2019, 2020b), and even in the effective discrimination of yeast strains and their growth phase monitoring through the alcoholic fermentation process (Puxeu et al., 2015). These approaches can be used for the assessment of individual time points (a measurement) and also to assess the quality of a set of measurements. In the latter case, several PCA models are developed and compared by using, for example, their loadings.

Since PCA loadings capture the chemical information of the process, Muncan et al. proposed a dissimilarity index (DI) to compare loadings of a yogurt fermentation process using a PCA model (Muncan et al., 2021). In this way, it was possible to distinguish and visualize three stages of the process related to the physicochemical properties of the yogurt matrix.

In this work, we present a multivariate statistical process control (MSPC) new statistic based on a novel dissimilarity index of NOC fermentations which, for the first time, is proposed to early detect process deviations. This variant of the DI consists of using an evolving window approach, which has been developed as a tool to monitor the progression of a biotechnological process. A portable attenuated total reflectance-Fourier transform infrared (ATR-FTIR) spectrometer was used to perform at-line and non-destructive measurements throughout the process. Three different scenarios that can lead to a deviation in the fermentations were tested: sudden changes in temperature, nitrogen deficiency at the start of fermentation, and a combination of both.

Materials and Methods

Samples and Fermentation Characteristics

The samples were obtained from small-scale alcoholic fermentations (microfermentations) of grape must carried out under different conditions. Specifically, a commercial and concentrated white grape must (Juan Soler S.A., Cuenca, Spain) was diluted with Milli-Q water to a final sugar concentration of 200 $g{\cdot}L^{-1}$, and, for each microfermentation, 1.5 L of diluted must was transferred into 2 L glass vessels for fermentation. Then, to start the alcoholic fermentation process, each must sample was inoculated randomly with $3{\cdot}10^6$ $CFU{\cdot}mL^{-1}$ of *Saccharomyces cerevisiae* Viniferm Revelación (Agrovin S.A., Ciudad Real, Spain), following the manufacturer instructions for rehydration of the dry yeast. Different fermentation conditions regarding the initial yeast assimilable nitrogen (YAN) concentration and temperature during the process were applied and are summarized in Table 1 (together with the abbreviations used in the text).

YAN was adjusted for NOC, TEM1, and TEM2 fermentations using Actimax Bio* (Agrovin, Ciudad Real, Spain) and ENOVIT® (SPINDAL S.A.R.L. Gretz

Table 1 Experimental conditions for the different types of fermentation carried out

Type of fermentation	Addition of *N* at the beginning	Temperature
NOC Normal operation condition	Yes	Constant at 20 °C
NDef Nitrogen deficit	No	Constant at 20 °C
TEM1 Applied temperature gradient 1	Yes	Gradient (Fig. 1a)
TEM2 Applied temperature gradient 2	Yes	Gradient (Fig. 1b)
NDT Nitrogen deficit and applied temperature gradient 2	No	Gradient (Fig. 1b)

Armainvilliers, France) at a dosage of 0.3 $g \cdot L^{-1}$ each, to ensure proper fermentation performance. The initial YAN concentration was 120 $mg \cdot L^{-1}$, and after the adjustment, YAN increased to 232 $mg \cdot L^{-1}$.

NOC and NDef fermentations were kept at a constant temperature of 20 °C throughout alcoholic fermentation. Two temperature gradients, shown in Fig. 1, were applied to TEM1, and TEM2 and NDT fermentations, respectively.

Two experimental plans were carried out (fermenting in different conditions at the same moment (diagram in Figure S1 and Table 2)): the first consisting in 6 NOC, 4 NDef, and 4 TEM1 fermentations and the second consisting in 6 NOC, 4 TEM2, and 4 NDT fermentations. All fermentations belonging to the same set were done at the same moment, but each fermentation was prepared randomly within each set.

To follow the evolution of the different alcoholic fermentations, each of the samples were randomly and periodically monitored (exact times are specified in Sect. 2.2) by measuring their density and pH, using a portable electronic densimeter (Densito2Go, Mettler Toledo, USA) and a portable pH-meter with a 201 T electrode (7 + series portable pH-meter, XS Instruments, Italy), respectively. Both instruments were calibrated daily using reference standards. Alcoholic fermentation was considered finished when density was less than 0.995 $g \cdot L^{-1}$. This value was reached between 7 and 9 days depending on the type of fermentation.

Spectroscopic Measurements

Infrared spectra were acquired according to a previously established methodology (Schorn-García et al., 2021), using a portable 4100 ExoScan FTIR spectrometer (Agilent, California, USA) equipped with a spherical ATR sampling interface with a diamond crystal window. The spectroscopic range covered from 4000 to 850 cm^{-1}, and spectra were recorded at a resolution of 8 cm^{-1} and 32 scans, implying the measurement of the signal at 845 wavenumbers. To eliminate the interference due to variations in environmental conditions, an air-background spectrum was collected before each sample measurement. Before the sampling of each of the fermentations, these were homogenized by gentle orbital stirring of the containers. After that, a sample of 1.5 mL was randomly collected and centrifuged at 10,000 rpm for 10 min to avoid the scattering effect in the spectroscopic measurements due to the presence of microorganisms. Each sample was analyzed in triplicate by placing successively three different drops of the sample on the crystal and recording the spectrum. The spectra were collected using Microlab PC software (Agilent, California, USA) and saved as.spc files. The average of the three measurements was used for further data analysis. The spectra were collected at the same times of the day, covering 12 daily hours of the process and sampling every 4 h (see, e.g., in Fig. S2). However, to better characterize the applied temperature gradients, one sample per hour was taken in NOC, TEM1, TEM2, and NDT. The details of the sampling points and matrix dimensions are shown in Table 2.

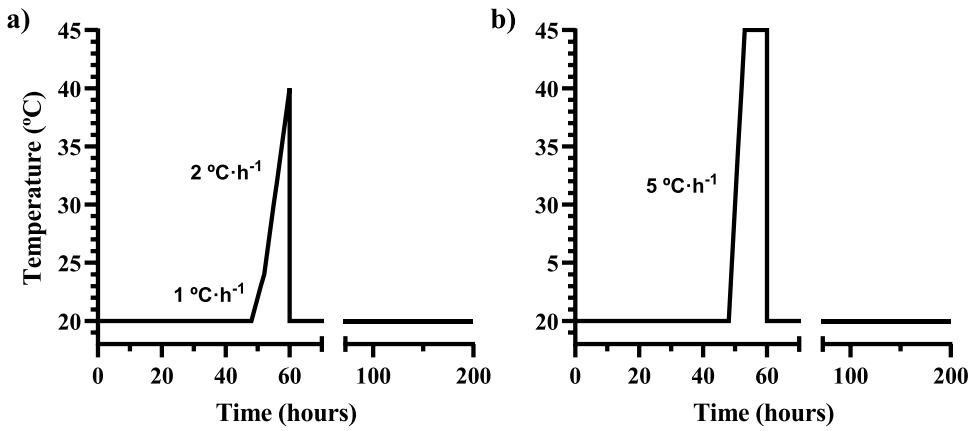

Fig. 1 Temperature gradient applied to **a** TEM1 fermentations and **b** TEM2 and NDT fermentations

Table 2 Overview of replicates, sampling points, and data matrix dimensions

Type of fermentation	Number of replicates	Sampling points	3D matrix dimension (replicates x samplings x wavenumbers)	Unfolded matrix
NOC	12	42	12×42×845	504×845
NDef	4	34	4×34×845	136×845
TEM1	4	42	4×42×845	168×845
TEM2	4	42	4×42×845	168×845
NDT	4	42	4×42×845	168×845

To maximize information and enhance small peaks, spectra were preprocessed using Savitzky-Golay second derivative (15 points and 2 order polynomial) and standard normal variate. Finally, spectra were mean centered.

Multivariate Statistical Process Control

A preliminary PCA model was built using the NOC spectra, in order to model spectroscopic information of the alcoholic fermentation. Next, three multivariate statistical process control approaches were tested: T^2, Q residuals, and score charts. The capability of the PCA model to detect deviations during the process using the defined reduced space was evaluated in each approach by projecting the different deviated fermentations. For T^2 and Q residuals, a 95% upper confidence limit was calculated using the NOC spectra, as defined in Cavaglia et al. (2020a). In the case of scores, an acceptance interval (upper and lower limits) was built as ± 2.201 standard deviations of the scores of the first principal component (Student's t for 11 degrees of freedom and 95% confidence level).

Dissimilarity Index

The dissimilarity index (Eq. 1) proposed by Muncan et al. (2021) is based on the absolute value of the inner product between the first loading of each model and the first loading of the initial model (Muncan et al., 2021).

$$A_i = 1 - \left|\mathbf{p}_i^{T}\mathbf{p}_0\right| \quad (1)$$

where A_i is the dissimilarity index for model i, and $\left|\mathbf{p}_i^{T}\mathbf{p}_0\right|$ is the inner product (in absolute value) of the transposed loading of the first principal component for model i and a reference loading (previous time model or model 0). This dimensionless parameter ranges from zero to one, with zero indicating that the loadings are identical and one indicating that they are orthogonal.

The DI was originally proposed using a moving-window approach, allowing to compare each part of the process with the preceding one in such a way that three process stages of the yogurt fermentation were distinguished. In the proposed index, five process times are selected, and the loading is compared with that of five previous process times, so that the comparison between the loading and the reference loading moves along the process until the whole process is considered.

Evolving Window Dissimilarity Index

The first step of the proposed approach involved the study of NOC fermentations. NOC alcoholic fermentations were monitored using evolving window principal component analysis (EWPCA) (Fig. 2). This method calculates PCA models in increasing time intervals, allowing including the entire evolution of the process up to a specific sampling time and giving equal weight to each part of the process, in contrast to the moving window approach, which only takes into account local parts of the process (de Oliveira et al., 2017). The first loading of each model was extracted and used to calculate the evolving window dissimilarity index (EWDI) along the fermentation process (Eq. 2).

$$DI_t = 1 - \left|\left(\mathbf{p}_{\text{Model n}}\right)^{T} \cdot \left(\mathbf{p}_{\text{Model 0}}\right)\right| \quad (2)$$

In Fig. 2, model 0 represents the start of fermentation, while model k represents the model spanning the entire fermentation. The initial window (i.e., the time window of model 0) was optimized, using different initial time gaps (the considered intervals, 0 to n, were between 0 and 24 h and 0 and 36 h). The loading extracted from model 0 was then used as the reference loading for NOC fermentations ($\mathbf{p}_{\text{Model 0}}$ in Eq. 2) and the evolving window dissimilarity index was calculated for all NOC fermentations (each time interval is considered in $\mathbf{p}_{\text{Model n}}$). The NOC dissimilarity curves were used to build acceptance interval calculated as the ± 2.201 standard deviations (Student's t for 11 degrees of freedom and 95% confidence level). Student's t was used since normal distribution of the EWDI was assumed.

After optimization of model 0 for NOC fermentations, the EWDI was calculated for all the other fermentations deviated from normal conditions (NDef, TEM1, TEM2, and

Fig. 2 Scheme of the evolving approach used to calculate the evolving window dissimilarity index, from time 0 to time *k*

NDT). The loading extracted from model 0 of NOC fermentations was also used as the reference loading ($\mathbf{p}_{\text{Model 0}}$ in Eq. 2) for all other fermentations that were to be compared.

ANOVA-simultaneous Component Analysis (ASCA)

Analysis of variance (ANOVA)-simultaneous component analysis (ASCA) was used to decompose the sources of variability influencing the data. ASCA is a multivariate extension of ANOVA, which decomposes the variation in the data into the main effects and their binary combinations according to a predefined experimental design (Smilde et al., 2005). In this study, three variability factors were considered: (1) to which set of batches the fermentation belonged (experiment factor), (2) whether or not fermentation was subjected to a temperature gradient, and (3) whether or not the fermentation had sufficient YAN at the beginning of alcoholic fermentation; and the interactions between them. ASCA was applied to the EWDI curves, obtaining as many EWDI curves as fermentation batches used (28 fermentations and 34 EWDI values each, to use the common times between them).

Results and Discussion

Control Charts Based on PCA

Classical MSPC approaches were tested and used as reference for EWDI performance evaluation. *Q* residuals and Hotelling T^2 charts were not useful to detect sluggish fermentations as they were not detected as outliers at any moment of the process. This may be due to the fact that the deviations caused in the process are related to the kinetics of the fermentation (Urtubia et al., 2008), which causes the NOC and deviated samples have similar spectroscopic features but are not temporarily aligned. In the case of the score control chart approach, all sluggish fermentations were successfully detected as deviated at different time intervals. NDef scores were significantly different from NOC scores from 56 to 168 h, as NDef fermentations evolve slower than NOC fermentations (see, e.g., for NDef in Fig. 3). For the deviations related to temperature gradients, TEM1 and TEM2, they were detected as outliers from 56 to 80 h and from 52 to 176 h, respectively. Finally, NDT fermentation was detected as outlier from 60 h onwards.

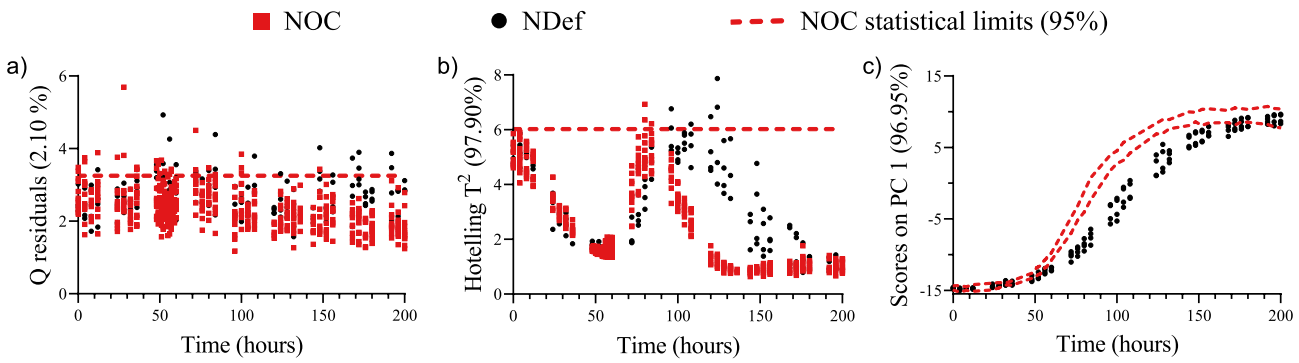

Fig. 3 **a** *Q* residuals, **b** Hotelling T^2, and **c** scores of the first principal component versus time. Red dots represent fermentations under normal operating conditions (NOCs), the black dots represent the fermentations that started with a nitrogen deficit (NDef), and the red dashed lines are the statistical limits for each of the monitoring metrics

Optimization of the Evolving Window Dissimilarity Index

The moving-window approach proposed to monitor yogurt fermentation (Muncan et al., 2021) did not perform well in the case of wine alcoholic fermentation. An erratic evolution (between 0 and 1) due to small differences between consecutive time intervals did not allow capturing all the useful information about the process. Thus, an evolving window approach was tried with good results after optimization. The optimization of the EWDI was performed by calculating the EWDI values of NOC spectra. The EWDI was calculated using the first PC loading, since in the PCA of the data of alcoholic wine fermentation the first PC collects the main information of the process (see Fig. S3 and (Schorn-García et al., 2021)). Furthermore, a different initial number of sampling points included in the reference PCA (model 0) was tested (5 to 8 sampling points, which include spectra from 0 to 24, 28, 32, or 36 h). An overview of the different EWDI evolutions based on the number of sampling points included in model 0 is shown in Fig. 4.

The EWDI evolution over time when considering 24 (Fig. 4a) and 28 (Fig. 4b) h in model 0 was not useful due to a great increase in the EWDI value for the first sampling points, followed by a stabilization of the value. This behavior did not allow studying the fermentation process, since after a certain point no significant differences were found between the EWDI values. However, the evolution over time of the EWDI considering 32 (Fig. 4c) or 36 (Fig. 4d) h in the model 0 showed better results, probably due to the inclusion of the early stages of tumultuous fermentation (phase of the process with the highest sugar-to-ethanol transformation ratio). Thus, the 36-h model 0 showed a better evolution in terms of sensitivity for the first sampling points, so this time was chosen to obtain the reference loading. By taking a wide enough window at the beginning of the process, small differences caused by microorganisms are minimized.

Regarding the loadings of model 0 (Fig. 4e and f), they showed that the important regions were between 3000 and 3500 cm^{-1}, which could be attributed to the O–H stretching vibrations of water and ethanol, and between 1000 and 1800 cm^{-1}, corresponding to the fingerprint region of the alcoholic fermentation (Bureau et al., 2019; Cozzolino, 2015). However, when more sampling points were considered (Fig. 4g and h) in model 0, the calculated loading underweighted the region between 3000 and 3500 cm^{-1} and incorporated a signal from 2300 to 2400 cm^{-1}, which could be attributed to O = C = O stretching, as carbon dioxide is released during alcoholic fermentation (Urtubia et al., 2008). This allowed us to focus on the alcoholic fermentation process in terms of the biochemical conversion of sugars into ethanol and also carbon dioxide.

Evolution of the Process and Deviations

The evolving window dissimilarity index of each sampling time was calculated for each fermentation type by grouping the spectra from each batch from the beginning to that sampling time and comparing the loadings of the first component with the loadings of the first component of model 0 for

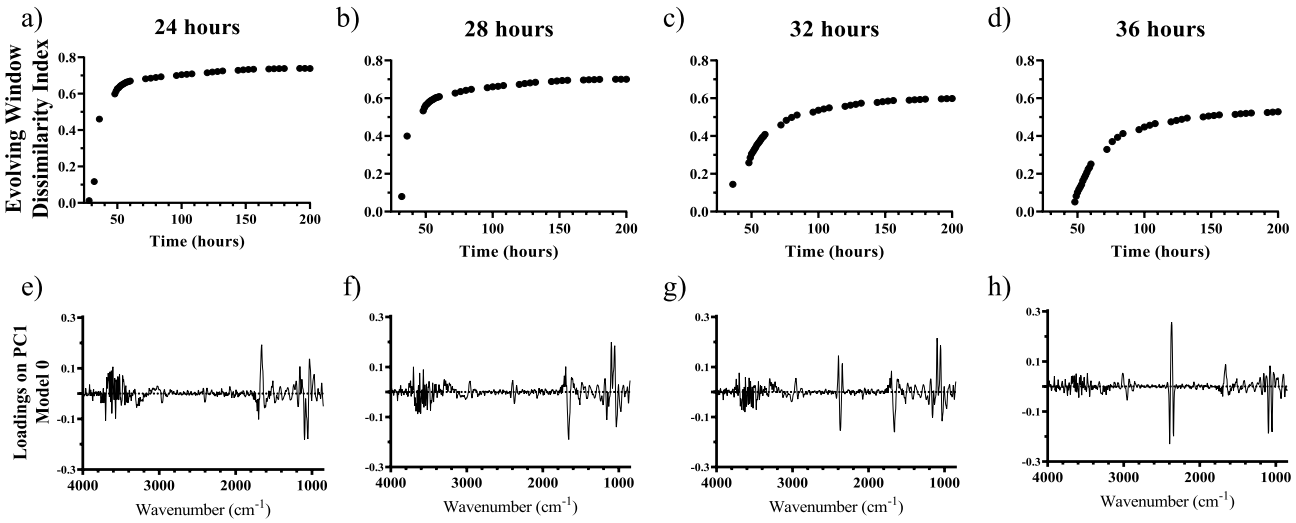

Fig. 4 **a**–**d** Evolving window dissimilarity index (EWDI) based on loading variation of NOC wine alcoholic fermentation, considering different time gaps for the reference loading (from 0 to 24 (**a**), 28 (**b**), 32 (**c**), or 36 (**d**) h). X-axis indicates the last sampling point included in the evolving window. **e**–**h** Reference loading used to calculate the EWDI, depending on the time gaps considered (from 0 to 24 (**e**), 28 (**f**), 32 (**g**), or 36 (**h**) h)

NOC samples. For example, there were 12 NOC fermentations, so for hour 48 (first EWDI value in Fig. 5) the loading of the first PC of the PCA model obtained with a matrix of size 108 × 845 (9 sampling times × 12 microfermentations batches × 845 wavenumbers) was compared to the loading of the first PC of model 0 of dimension 96 × 845 (8 sampling times × 12 microfermentations batches × 845 wavenumbers). The EWDI evolution over time for each fermentation type is shown in Fig. 5.

In all types of fermentation, a noticeable increase of the EWDI was observed between 48 and 100 h. This time frame coincided with the tumultuous phase of fermentation, during which the rate of glucose consumption was the highest. When sugars are converted to ethanol at the maximum rate, EWDI values also increase rapidly. After 100 h, the increase in EWDI slowed down and continued with a slight increase until the end of fermentation, which occurred around 200 h (when all types of fermentation finished). In general, the evolution of EWDI during fermentation provided valuable insights into the progress of the process, making it a useful tool for monitoring fermentation. Using the loading of the first principal component, related to the conversion of sugars into ethanol, allowed the monitoring of the kinetics of the process.

The fermentation types that underwent a temperature change (TEM1, TEM2, and NDT), showed a similar upward trend between 48 and 60 h, when the temperature gradient was applied. This trend could be explained as yeasts have their optimal temperature range between 16 and 30 °C (Ribereau-Gayon et al., 2006). At the beginning of the temperature gradient, yeasts had a more optimal temperature (closer to 30 °C), which allows them to increase their metabolic activity. Afterwards, the upper limit in their optimal temperature was surpassed affecting their metabolism. This explains the slower EWDI evolution after the temperature gradient. NDef showed a slower evolution over time; however, NDef and NDT ended the fermentation with a higher EWDI compared to NOC fermentation. The slower fermentation rate at the beginning would be explained by the lower amount of YAN available to carry out yeast metabolism properly (Martínez-Moreno et al., 2012). NDT showed an intermediate behavior of TEM2 and NDef, which may explain its EWDI evolution over time.

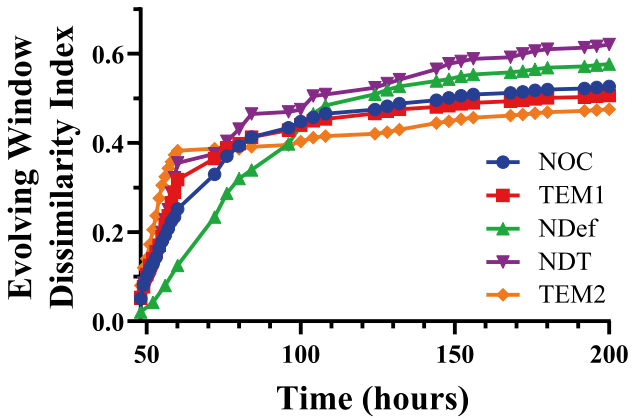

Fig. 5 Evolving window dissimilarity index based on loading variation of wine alcoholic fermentation with different characteristics (blue circles, normal operation conditions (NOCs); red squares, fermentations that suffered a temperature gradient depicted in Fig. 1a (TEM1); green triangles, fermentations that started with a nitrogen deficit (NDef); purple inverted triangles, fermentations that started with a nitrogen deficit and suffered a temperature gradient depicted in Fig. 1b (NDT); orange rhombi, fermentations that suffered a temperature gradient depicted in Fig. 1b (TEM2)). X-axis indicates the last sampling point included in the evolving window

3.4. Evolving Window Dissimilarity Index Control Chart

As discussed above, the NOC spectra of the first 36 h was used to obtain the reference loading (first loading of model 0), calculated as the loading of the first PC (shown in Fig. 4h). The NOC EWDI curves were used to calculate 95% acceptance interval (average of 12 EWDI NOC curves ± 2.201 standard deviations) (red dotted lines in Fig. 6).

The NOC EWDI upper and lower acceptance intervals showed a greater difference up to 100 h due to the great fermentation activity during this period. In fact, from 48 to 100 h, the alcoholic fermentation process had the maximum rate of sugar consumption, and even slight differences between NOC batches resulted in increased acceptance interval. Then, from 100 h to the end of the process, the acceptance interval was much tighter as the fermentation process decreases in intensity. EWDI acceptance interval were validated with other NOC fermentation evolutions, showing the ability of this parameter to be used for monitoring this bioprocess. In each case, the EWDI was calculated and its value remained within the acceptance interval throughout the entire fermentation process. It is worth noting that, contrary to what other MSPC strategies may require, there is no requirement for process alignment because the EWDI comparison is carried out by using the model loadings.

However, despite the wider acceptance interval at the beginning, the proposed MSPC chart was able to detect sluggish fermentations. Figure 6a shows the evolution of EWDI for TEM1, where the control chart was able to detect all the batches outside the acceptance interval from 60 to 76 h. In this type of fermentation, the EWDI showed out-of-control values shortly after the temperature rise reached its maximum at some later sampling points. However, from 80 h onwards, TEM1 had a EWDI considered under control, and this behavior can also be observed in Fig. 4, where TEM1 had EWDI values similar to NOC at the end of the process. The time interval considered as out-of-control (60 to 76 h) for TEM1 was relatively short, with only three sampling points being affected.

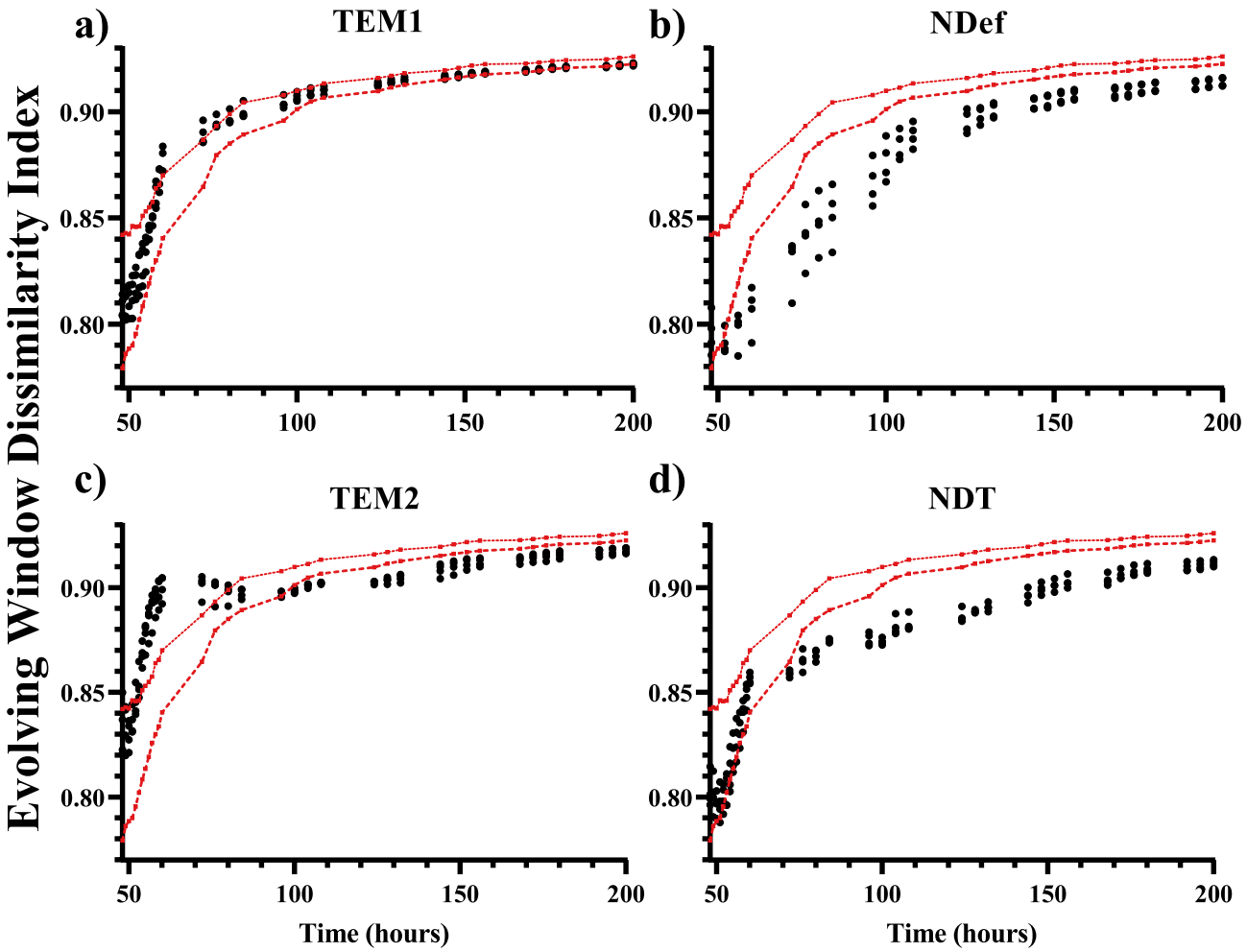

Fig. 6 Evolving window dissimilarity index (EWDI) control charts based on loading variation of wine alcoholic fermentation. Red lines represent mean EWDI values for NOC fermentation and red dotted lines represent 95% acceptance intervals calculated based on EWDI curves of the twelve NOC fermentations (average ± 2.201 standard deviation). The different charts represent the values of EWDI curves for different types of fermentation: **a** fermentations that suffered a temperature gradient depicted in Fig. 1a (TEM1); **b** fermentations that started with a nitrogen deficit (NDef); **c** fermentations that suffered a temperature gradient depicted in Fig. 1b (TEM2); **d** fermentations that started with a nitrogen deficit and suffered a temperature gradient depicted in Fig. 1b (NDT). X-axis indicates the last sampling point included in the evolving window

In the case of NDef (shown in Fig. 6b), the control chart was able to detect all out-of-control batches starting at 53 h. This sluggish fermentation was intentionally induced by creating a nitrogen deficit, which can cause a malfunction in the metabolism of yeast (Martínez-Moreno et al., 2012). Figure 6c shows the evolution of EWDI for TEM2. In this case, each batch was detected as out-of-control starting at 53 h, with the exception of one particular time period where the EWDI values "crossed" the acceptance interval. The temperature variation applied between 48 to 60 h was detected 5 h after its beginning, indicating the effectiveness of the MSPC chart in detecting process deviations at an early stage. NDT fermentations (shown in Fig. 6d) were a combination of nitrogen deficit and temperature gradient, resulting in intermediate behavior compared to sluggish fermentations caused by each factor separately. The evolution of NDT EWDI showed that these fermentation batches were identified as out-of-control later than the other deviations studied, due to the slow progress caused by the nitrogen deficit, which was compensated by an increase in temperature that allowed an increase in yeast metabolism. However, after 72 h, this type of sluggish fermentation remained out-of-control.

All deviations resulted in distinctive spectroscopic profiles in the final wines. This feature is particularly advantageous for assessing these deviations at any stage of the fermentation process, even when real-time process monitoring is not feasible. This is relevant for the monitoring alcoholic fermentation, because the effects of the corrective measures take time to manifest themselves in the behavior of the process, due to the prolonged nature of the fermentation process which spans several days.

Table 3 ASCA results for the EWDI curves, showing the percentage of variance (% effect) for each factor and the *p* value resulting of the permutation test. A *p*-value < 0.05 means the factor is significant

Factor	% Effect	*p*-value
Temperature gradient	23.97	0.0001
Nitrogen deficit	61.06	0.0001
Temperature gradient × nitrogen deficit	7.05	0.0004
Residual	7.92	

Study of the Variability of Sluggish Fermentation

To study the influence of the different problems that cause sluggish alcoholic fermentations and weight their contribution, an ASCA model was built. Since two groups of fermentations were performed (described in "Samples and Fermentation Characteristics" section), this factor (group) was evaluated in a previous model showing that it is not significant, and there are no differences between sets of experiments (data not shown). To build the ASCA model, all EWDI curves over time were used, i.e., 32 curves. Two factors were considered: the sudden change in temperature ("temperature gradient" factor) and the nitrogen deficit at the beginning of the fermentation ("nitrogen deficit" factor). The results of the ASCA model are summarized in Table 3.

The most relevant factor was whether or not the fermentation started with the adequate nitrogen content, as almost -thirds of the variance (61.06%) was attributed to the "nitrogen deficit" factor. The shape of the EWDI evolution curve was found to be more similar to the NDef than to the TEM2 deviations, which is in an indication of the importance of the factor. For this reason, it is necessary to guarantee the concentration of nitrogen (the minimum limit would depend on the concentration of sugar in the must) to ensure the end of fermentation and avoid the production of unwanted molecules (Lleixà et al., 2019; Torrea et al., 2011). These ASCA results highlighted the importance of measuring YAN to ensure a correct development of the alcoholic fermentation by yeast from the beginning of the process. The "temperature gradient" factor also showed a significant impact in the process evolution, with a % effect close to 24%. This problem can be associated with inadequate temperature control, malfunctioning cooling jackets or high external temperatures that could cause sudden temperature increases. Furthermore, given that alcoholic fermentation is an exothermic process, even in the absence of external factors, the process itself can cause the temperature to rise if not properly controlled. This can have a negative effect on the development of the fermentation and on the quality of the final product, due to the loss of aromas as a consequence of the increased volatilization of volatile compounds, as well as by the stress of the yeasts, which could synthesize unwanted molecules (Torija et al., 2003; Woo et al., 2014).

ASCA results for each factor are depicted in Fig. 7, which displays the scores of the first simultaneous component. Figure 7a shows the score values of the "temperature gradient" submodel for each sample. The scores are colored according to the temperature gradient applied to the process (blue circles for a constant temperature along the process, red squares for processes that suffered a temperature gradient as depicted in Fig. 1a, and green triangles for processes that suffered a temperature gradient as depicted in Fig. 1b). Two main groups can be seen in the first simultaneous component:

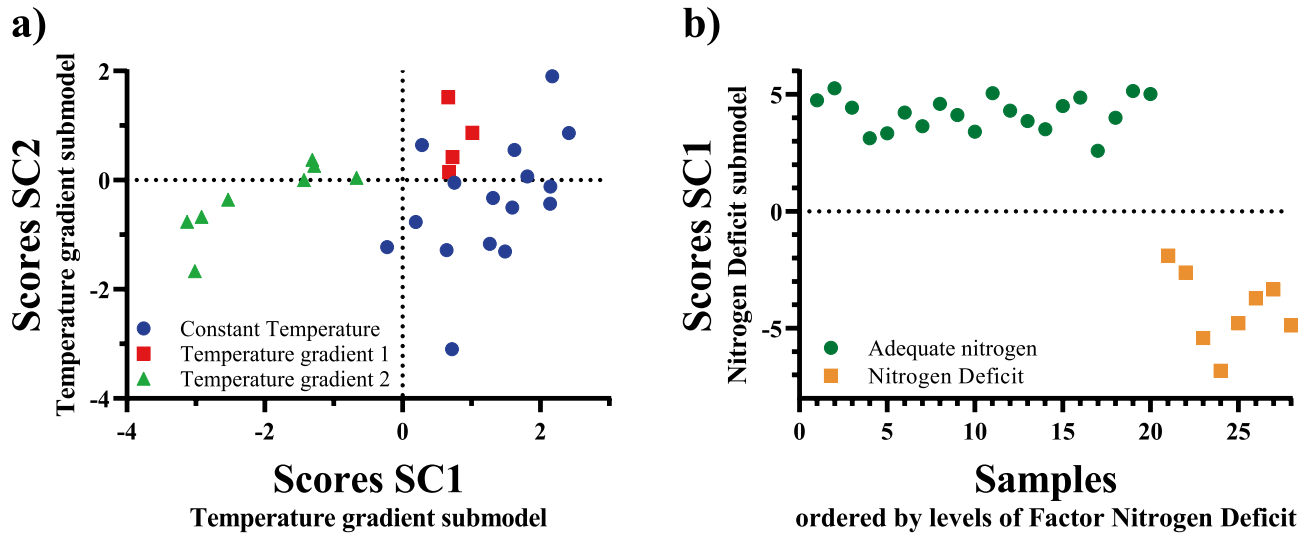

Fig. 7 ASCA results on the EWDI curves. **a** Scores of the first and second simultaneous component of the temperature gradient factor submodel and **b** score of the first simultaneous component of the nitrogen deficit factor submodel, where the samples are ordered by the levels of each factor. Dotted lines are used to visualize the center of each PC

NOC, TEM1, and NDef have positive values in this component, while TEM2 and NDT have negative values. This could be explained because TEM1 showed, based on the results of the "Evolution of the Process and Deviations" and "Optimization of the Evolving Window Dissimilarity Index" sections, similar behavior to NOC in terms of EWDI evolution, and that the second temperature gradient had a greater impact on the course of alcoholic fermentation and therefore in the evolution of EWDI over time.

Figure 7b shows the score value of the "nitrogen deficit" submodel for each sample, colored according to whether or not the process had a nitrogen deficit at the beginning of fermentation (an adequate nitrogen content in green and a deficit of nitrogen in orange). In the first simultaneous component, two main groups can be observed. NOC, TEM1, and TEM2 fermentations had positive values, while the NDef and NDT fermentations had negative values. The % effect of nitrogen deficit revealed by ASCA highlighted the importance of an adequate nitrogen content and resulted in a clear separation of score values between the groups.

Conclusions

The dissimilarity index (DI) is a process control parameter that can accurately describe the progression of fermentation in real time. In this study, a modified DI was proposed, the EWDI, and used to examine sluggish alcoholic fermentations and observe their development. The results have shown that the EWDI can be used to create a control chart based on data from normal operating conditions. Furthermore, the confidence limits of the control chart can be used to detect sluggish fermentations, related to the kinetics of the fermentation, at an early stage. This is particularly important because early detection allows timely intervention to resolve any issues that may arise and therefore increases the chances of maintaining product quality.

In conclusion, the EWDI appears to be an effective tool for process control, allowing real-time monitoring and early detection of potential deviations. Additionally, the effect of different unwanted conditions affecting process kinetics have been studied and decomposed showing that EWDI evolution over time could indicate which kind of deviation is taking place and the importance of nitrogen supplementation at the beginning of the process. Further research would be developed to investigate the recovery of deviation using EWDI control charts.

Supplementary Information The online version contains supplementary material available at https://doi.org/10.1007/s11947-023-03266-z.

Acknowledgements The authors would like to thank the Wine Biotechnology group for the yeast strain used in this experiment. The authors would like to thank Víctor Maixé for his design of the fermentation container cover. The authors would like to thank Candela Ruiz-de-Villa for helping to set up the beginning of each experiment. Graphical abstract made using BioRender.com.

Author Contribution DS-G: Methodology, software, investigation, validation, visualization, writing—original draft. JE: Software, validation, writing—original draft. OB: Funding acquisition. LA: Resources, project administration. RB: Validation, writing (review and editing), funding acquisition. MM: Conceptualization, validation, writing—review and editing. BG: Conceptualization, investigation, validation, formal analysis, writing—review and editing.

Funding Open access funding provided by Università degli Studi dell'Insubria within the CRUI-CARE Agreement. Grant PID2019-104269RR-C33 funded by MCIN/AEI/10.13039/501100011033. This publication has been possible with the support of the Secretaria d'Universitats i Recerca del Departament d'Empresa i Coneixement de la Generalitat de Catalunya (2020 FISDU 00221; Schorn-Garcia, D.). Grant URV Martí i Franqués—Banco Santander (2021PMF-BS-12).

Data Availability The data that support the findings of this study are available from the authors upon reasonable request.

Declarations

Conflict of Interest The authors declare that they have no known competing financial or personal relationships that could have appeared to influence the work reported in this paper.

References

Alexandre, H., & Charpentier, C. (1998). Biochemical aspects of stuck and sluggish fermentation in grape must. *Journal of Industrial Microbiology and Biotechnology, 20*(1), 20–27. https://doi.org/10.1038/SJ.JIM.2900442

Bao, Y., Liu, F., Kong, W., Sun, D. W., He, Y., & Qiu, Z. (2014). Measurement of soluble solid contents and pH of white vinegars using VIS/NIR spectroscopy and least squares support vector machine. *Food and Bioprocess Technology, 7*(1), 54–61. https://doi.org/10.1007/S11947-013-1065-0

Bureau, S., Cozzolino, D., & Clark, C. J. (2019). Contributions of Fourier-transform mid infrared (FT-MIR) spectroscopy to the study of fruit and vegetables: A review. *Postharvest Biology and Technology*, *148*, 1–14. https://doi.org/10.1016/j.postharvbio.2018.10.003

Cavaglia, J., Giussani, B., Mestres, M., Puxeu, M., Busto, O., Ferré, J., & Boqué, R. (2019). Early detection of undesirable deviations in must fermentation using a portable FTIR-ATR instrument and multivariate analysis. *Journal of Chemometrics, 33*, e3162. https://doi.org/10.1002/cem.3162

Cavaglia, J., Schorn-García, D., Giussani, B., Ferré, J., Busto, O., Aceña, L., et al. (2020a). Monitoring wine fermentation deviations using an ATR-MIR spectrometer and MSPC charts. *Chemometrics and Intelligent Laboratory Systems, 201*, 104011. https://doi.org/10.1016/j.chemolab.2020.104011

Cavaglia, J., Schorn-García, D., Giussani, B., Ferré, J., Busto, O., Aceña, L., et al. (2020b). ATR-MIR spectroscopy and multivariate analysis in alcoholic fermentation monitoring and lactic acid bacteria spoilage detection. *Food Control*, *109*, 106947. https://doi.org/10.1016/j.foodcont.2019.106947

Cozzolino, D. (2015). Sample presentation, sources of error and future perspectives on the application of vibrational spectroscopy in the wine industry. *Journal of the Science of Food and Agriculture, 95*(5), 861–868. https://doi.org/10.1002/jsfa.6733

Cozzolino, D. (2016). State-of-the-art advantages and drawbacks on the application of vibrational spectroscopy to monitor alcoholic fermentation (beer and wine). *Applied Spectroscopy Reviews, 51*(4), 282–297. https://doi.org/10.1080/05704928.2015.1132721

Cozzolino, D. (2022). Advantages, opportunities, and challenges of vibrational spectroscopy as tool to monitor sustainable food systems. *Food Analytical Methods, 15*(5), 1390–1396. https://doi.org/10.1007/s12161-021-02207-w

de Oliveira, R. R., Pedroza, R. H. P., Sousa, A. O., Lima, M. G., & de Juan, A. (2017). *Process modeling and control applied to real-time monitoring of distillation processes by near-infrared spectroscopy.* https://doi.org/10.1016/j.aca.2017.07.038

Food Drink, E. (2022). *Data & trends EU food and drink industry*. Belgium.

Grassi, S., Alamprese, C., Bono, V., Casiraghi, E., & Amigo, J. M. (2014). Modelling milk lactic acid fermentation using multivariate curve resolution-alternating least squares (MCR-ALS). *Food and Bioprocess Technology, 7*(6), 1819–1829. https://doi.org/10.1007/S11947-013-1189-2

Hernández, G., León, R., & Urtubia, A. (2016). Detection of abnormal processes of wine fermentation by support vector machines. *Cluster Computing, 19*, 1219–1225. https://doi.org/10.1007/s10586-016-0594-5

Jenzsch, M., Bell, C., Buziol, S., Kepert, F., Wegele, H., & Hakemey, C. (2018). Trends in process analytical technology: Present state in bioprocessing. In B. Kiss, U. Gottschal, & M. Pohlscheidt (Eds.), *New Bioprocessing Strategies: Development and Manufacturing of Recombinant Antibodies and Proteins* (1st Editio., pp. 211–252). Switzerland: Springer International Publishing.

Lleixà, J., Martín, V., Giorello, F., Portillo, M. C., Carrau, F., Beltran, G., & Mas, A. (2019). Analysis of the NCR mechanisms in Hanseniaspora vineae and Saccharomyces cerevisiae during winemaking. *Frontiers in Genetics*, *10*, 747. https://doi.org/10.3389/FGENE.2018.00747/BIBTEX

Martínez-Moreno, R., Morales, P., Gonzalez, R., Mas, A., & Beltran, G. (2012). Biomass production and alcoholic fermentation performance of Saccharomyces cerevisiae as a function of nitrogen source. *FEMS Yeast Research, 12*(4), 477–485. https://doi.org/10.1111/j.1567-1364.2012.00802.x

Muncan, J., Tei, K., & Tsenkova, R. (2021). Real-time monitoring of yogurt fermentation process by aquaphotomics near-infrared spectroscopy. *Sensors (switzerland), 21*(1), 1–18. https://doi.org/10.3390/s21010177

Nieto-Ortega, S., Mas García, S., Melado-Herreros, Á., Foti, G., Olabarrieta, I., & Roger, J. M. (2023). Multivariate curve resolution applied to near infrared spectroscopic data acquired throughout the cooking process to monitor evolving Béchamel sauces. *Food and Bioprocess Technology, 16*(4), 881–896. https://doi.org/10.1007/S11947-022-02972-4

Nomikos, P., & MacGregor, J. F. (1995). Multi-way partial least squares in monitoring batch processes. *Chemometrics and Intelligent Laboratory Systems, 30*(1), 97–108. https://doi.org/10.1016/0169-7439(95)00043-7

Puxeu, M., Andorra, I., & De Lamo-Castellví, S. (2015). Monitoring Saccharomyces cerevisiae Grape must fermentation process by attenuated total reflectance spectroscopy. *Food and Bioprocess Technology, 8*(3), 637–646. https://doi.org/10.1007/S11947-014-1435-2

Ribereau-Gayon, P., Dubourdieu, D., Doneche, B., & Lonvaud, A. (2006). *Handbook of enology: The microbiology of wine and vinifications: Second Edition*. *Handbook of Enology: The Microbiology of Wine and Vinifications: Second Edition* (Vol. 1). wiley. https://doi.org/10.1002/0470010363

Schorn-García, D., Cavaglia, J., Giussani, B., Busto, O., Aceña, L., Mestres, M., & Boqué, R. (2021). ATR-MIR spectroscopy as a process analytical technology in wine alcoholic fermentation – A tutorial. *Microchemical Journal, 166*, 106215. https://doi.org/10.1016/j.microc.2021.106215

Smilde, A. K., Jansen, J. J., Hoefsloot, H. C. J., Lamers, R. J. A. N., van der Greef, J., & Timmerman, M. E. (2005). ANOVA-simultaneous component analysis (ASCA): A new tool for analyzing designed metabolomics data. *Bioinformatics, 21*(13), 3043–3048. https://doi.org/10.1093/bioinformatics/bti476

Torija, M. J., Rozès, N., Poblet, M., Guillamón, J. M., & Mas, A. (2003). Effects of fermentation temperature on the strain population of Saccharomyces cerevisiae. *International Journal of Food Microbiology, 80*(1), 47–53. https://doi.org/10.1016/S0168-1605(02)00144-7

Torrea, D., Varela, C., Ugliano, M., Ancin-Azpilicueta, C., Leigh Francis, I., & Henschke, P. A. (2011). Comparison of inorganic and organic nitrogen supplementation of grape juice – Effect on volatile composition and aroma profile of a Chardonnay wine fermented with Saccharomyces cerevisiae yeast. *Food Chemistry, 127*(3), 1072–1083. https://doi.org/10.1016/J.FOODCHEM.2011.01.092

U.S. Department of Health and Human Services, Food and Drug Administration. (2004). *Guidance for industry PAT — A framework for innovative pharmaceutical development, manufacuring, and quality assurance*. FDA official document.

Urtubia, A., Pérez-correa, J. R., Pizarro, F., & Agosin, E. (2008). Exploring the applicability of MIR spectroscopy to detect early indications of wine fermentation problems. *Food Control, 19*(1), 382–388. https://doi.org/10.1016/j.foodcont.2007.04.017

Woo, J. M., Yang, K. M., Kim, S. U., Blank, L. M., & Park, J. B. (2014). High temperature stimulates acetic acid accumulation and enhances the growth inhibition and ethanol production by Saccharomyces cerevisiae under fermenting conditions. *Applied Microbiology and Biotechnology, 98*(13), 6085–6094. https://doi.org/10.1007/S00253-014-5691-X/FIGURES/7

Ye, M., Yue, T., Yuan, Y., & Li, Z. (2014). Application of FT-NIR spectroscopy to apple wine for rapid simultaneous determination of soluble solids content, pH, total acidity, and total ester content. *Food and Bioprocess Technology, 7*(10), 3055–3062. https://doi.org/10.1007/S11947-014-1385-8